Title	Transport and thermodynamic properties of quasi-two-dimensional purple bronzes A0.9Mo6O17 (A=Na, K)
Author(s)	Xu, Xiaofeng; Bangura, A. F.; Niu, C. Q.; Greenblatt, M.; Yue, Song; Panagopoulos, Christos; Hussey, N. E.
Citation	Xu, X., Bangura, A. F., Niu, C. Q., Greenblatt, M., Yue, S., Panagopoulos, C., et al. (2012). Transport and thermodynamic properties of quasi-two-dimensional purple bronzes A0.9Mo6O17 (A=Na, K). Physical Review B, 85(19), 195101-.
Date	2012
URL	http://hdl.handle.net/10220/9315
Rights	

Transport and thermodynamic properties of quasi-two-dimensional purple bronzes $A_{0.9}Mo_6O_{17}$ (A = Na, K)

Xiaofeng Xu,[1,2,3] A. F. Bangura,[2,4] C. Q. Niu,[1] M. Greenblatt,[5] Song Yue,[6] C. Panagopoulos,[3] and N. E. Hussey[2]

[1]*Department of Physics, Hangzhou Normal University, Hangzhou 310036, China*

[2]*H. H. Wills Physics Laboratory, University of Bristol, Tyndall Avenue, BS8 1TL, United Kingdom*

[3]*Division of Physics and Applied Physics, School of Physical and Mathematical Sciences, Nanyang Technological University, 637371 Singapore*

[4]*RIKEN(The Institute of Physical and Chemical Research), Wako, Saitama 351-0198, Japan*

[5]*Department of Chemistry and Chemical Biology, Rutgers University, Piscataway, New Jersey 08854, USA*

[6]*Department of Physics, Jinan University, Guangzhou, China*

(Received 14 November 2011; revised manuscript received 26 March 2012; published 2 May 2012)

We report a comparative study of the specific heat, electrical resistivity, and thermal conductivity of the quasi-two-dimensional purple bronzes $Na_{0.9}Mo_6O_{17}$ and $K_{0.9}Mo_6O_{17}$, with special emphasis on the behavior near their respective charge-density-wave transition temperatures T_P. The contrasting behavior of both the transport and the thermodynamic properties near T_P is argued to arise predominantly from the different levels of intrinsic disorder in the two systems. A significant proportion of the enhancement of the thermal conductivity above T_P in $Na_{0.9}Mo_6O_{17}$, and to a lesser extent in $K_{0.9}Mo_6O_{17}$, is attributed to the emergence of phason excitations.

DOI: 10.1103/PhysRevB.85.195101 PACS number(s): 71.45.Lr, 72.15.Eb, 65.40.Ba, 72.15.Nj

I. INTRODUCTION

It is well known that in many low-dimensional compounds, Fermi surfaces are unstable against a Peierls instability below a critical temperature T_P. The mean-field description of this so-called charge-density-wave (CDW) state is characterized by the opening of the electronic gap at the Fermi level, accompanied by a softening in the phonon spectrum at $Q = 2k_F$, with k_F the Fermi wave vector. As first pointed out by Lee, Rice and Anderson,[1] this soft-phonon spectrum splits into two new modes of collective oscillations: one corresponds to opticlike amplitude mode and the other one to an acousticlike phase mode. This phase mode or phason existing at zero frequency in the ideal CDW compounds corresponds to the sliding motion of the CDW as proposed by Fröhlich.[2] In real materials, however, the phason excitations are gapped out primarily due to impurity pinning. While these gapped phason excitations may not contribute to the *charge* transport directly, they may still play a role in the *thermal* transport owing to the finite value of $d\omega/dq$ in their spectrum.

The quasi-two-dimensional (Q2D) purple bronzes $Na_{0.9}Mo_6O_{17}$ and $K_{0.9}Mo_6O_{17}$ undergo CDW transitions at $T_P \sim 80$ and 120 K, respectively, which has been confirmed by various probes such as electrical resistivity and magnetic susceptibility.[3] In $K_{0.9}Mo_6O_{17}$, diffuse x-ray scattering and electron diffraction experiments have also revealed the three nesting wave vectors of (a^*, 0, 0) and its symmetrical equivalents below T_P,[4] while scanning tunneling microscopy (STM) studies further observed the (2×2) superstructure imposed on the crystal lattice at low temperatures.[5] With regard to their crystal structures, these two compounds share a great deal of commonality, albeit with slight differences in symmetry, i.e., trigonal $P\bar{3}$ symmetry in $K_{0.9}Mo_6O_{17}$ versus monoclinic $C2$ symmetry in $Na_{0.9}Mo_6O_{17}$.[3] The main building block in both systems is the slabs of Mo-O corner-sharing polyhedra, consisting of four MoO_6 octahedral layers terminated on either side by a layer of MoO_4 tetrahedra. These slabs lie perpendicular to the c axis and are separated from each other by a layer of alkali metals. The MoO_4 tetrahedra in adjacent layers do not share corners, disrupting the Mo-O-Mo bonding along the c axis.[3] This layered structure is expected to lead to a Q2D electronic structure, as confirmed by dc transport measurements.[3]

The precise topology of the $Na_{0.9}Mo_6O_{17}$ Fermi surface (FS), as revealed by angle-resolved photoemission spectroscopy (ARPES),[6,7] remains controversial, with different ARPES groups claiming a FS topology that is either similar to[6] or distinct from[7] that of $K_{0.9}Mo_6O_{17}$. According to Breuer *et al.*,[7] there is only one electron pocket centered around the Γ point in $Na_{0.9}Mo_6O_{17}$, rather than the two pockets found in $K_{0.9}Mo_6O_{17}$. Moreover, while the FS of $K_{0.9}Mo_6O_{17}$ can be viewed as a combination of pairs of quasi-one-dimensional (Q1D) Fermi sheets which can be nested to one another by the so-called "hidden" nesting vectors,[8,9] Breuer *et al.* find no evidence for the 1D FS parallel to the ΓX direction in sodium purple bronze. These subtle yet important differences in the proposed electronic structure are supported, on a qualitative level at least, by the observation that the thermoelectric power $S(T)$ below T_P is dramatically different in the two systems;[10] while $S(T)$ in both systems decreases linearly with decreasing temperature toward zero at $T = T_P$, below T_P, $S(T)$ shows a large negative (positive) peak for A = Na (K), respectively, suggesting that the dominant carrier has an opposite sign in the two cases.

To gain further insight into the nature of the CDW formation in these two compounds, in particular the changes in the nature of their electronic and phononic subsystems at $T = T_P$, we present in this paper a comparative study of the specific heat, electrical resistivity, and thermal conductivity of $Na_{0.9}Mo_6O_{17}$ and $K_{0.9}Mo_6O_{17}$ over a broad temperature range above and below their respective CDW transitions. A number of key features are uncovered. First, the anisotropy of the electrical resistivity is found to be an order of magnitude higher than has been reported in the existing literature. Second,

in $Na_{0.9}Mo_6O_{17}$, the in-plane thermal conductivity $\kappa_{ab}(T)$ is found to decrease across the CDW transition, in marked contrast to the significant enhancement of $\kappa_{ab}(T)$ observed at T_P in $K_{0.9}Mo_6O_{17}$. Finally, in the heat-capacity data, a large λ-shape anomaly is observed in $K_{0.9}Mo_6O_{17}$, while in $Na_{0.9}Mo_6O_{17}$, the heat capacity exhibits a broad hump with no discernible feature at T_P. We argue here that the principal origin of these distinct physical responses in the two systems is the difference in their alkali-metal stoichiometry. We also reveal the possible manifestation of phason excitations in the thermal conductivity of these archetypal CDW bronzes above T_P.

II. EXPERIMENT

The single crystals used in this study were grown by electrolytic reduction of a melt of A_2CO_3-MoO_3 (A = Na,K) with an appropriate molar ratio. The details of the sample growth procedure are described elsewhere.[10–14] Good single crystallinity of the as-grown samples was confirmed by a single-crystal x-ray diffractometer. The plateletlike samples were then cut into bar shapes of appropriate geometry for in-plane and out-of-plane transport measurements. The resistivity of each sample was measured with a standard four-probe ac lock-in detection technique.

For the thermal conductivity measurements, we developed a zero-field apparatus housed in a ^{4}He flow cryostat that covers the temperature range $10 < T < 300$ K. We employed a modified steady-state method, shown schematically in Fig. S2 of Ref. 15, in which a temperature gradient, measured using a differential thermocouple, is set up across the sample through a pair of calibrated heat links attached to each end. The sample is suspended by the free ends of the heat links between two platforms that are weakly coupled to the heat bath. Each platform houses a heater that enables a temperature gradient to be set up across the sample in both directions at a fixed heat-bath temperature. The heat links are also differential thermocouples that allow the heat flowing into and out of the sample to be measured simultaneously in order to determine the heat loss across the sample in steady state.

The heat-capacity measurements were performed in a commercial Quantum Design PPMS system. The measurements were done on a large single-crystal piece of $Na_{0.9}Mo_6O_{17}$ (of 2.495 mg in weight), and two pieces of single-crystalline $K_{0.9}Mo_6O_{17}$ (total weight 1.190 mg). The heat capacity of the addenda was determined in a separate run and subtracted from the total heat capacity. In the $C_p(H)$ measurements, a static magnetic field of 14 T was applied along the crystallographic c axis.

III. RESULTS

Figure 1 summarizes both the in-plane (ρ_{ab}) and interplane (ρ_c) resistivities of our $Na_{0.9}Mo_6O_{17}$ and $K_{0.9}Mo_6O_{17}$ single crystals. Overall, the temperature dependence in each case is in good agreement with what has been reported previously.[3,10] Specifically, both $\rho_{ab}(T)$ and $\rho_c(T)$ are approximately T linear at high temperatures, then pass through a well-defined minimum around $T = T_P$. At the lowest temperature studied, both systems develop a second upturn that is larger in the A = Na bronze. In both cases, the zero-temperature resistivity tends toward a finite value, confirming that these CDW transitions are metal-metal transitions. As the resistivity minima at T_P in both systems are rather broad, we use their derivatives $(d \ln \rho)/dT$, plotted in Fig. 2, to define the onset of the CDW transition, as is the norm.[3] From both $(d \ln \rho_{ab})/dT$ and $(d \ln \rho_c)/dT$, deep minima are identified at ∼80 and ∼100 K for $Na_{0.9}Mo_6O_{17}$ and $K_{0.9}Mo_6O_{17}$, respectively, in good agreement with previous studies.[3] Evidently, the width of the derivative minimum at $T = T_P$ is much sharper in $K_{0.9}Mo_6O_{17}$ than in $Na_{0.9}Mo_6O_{17}$, suggestive of a lower intrinsic disorder level in the former. We shall return to this point in the Discussion section.

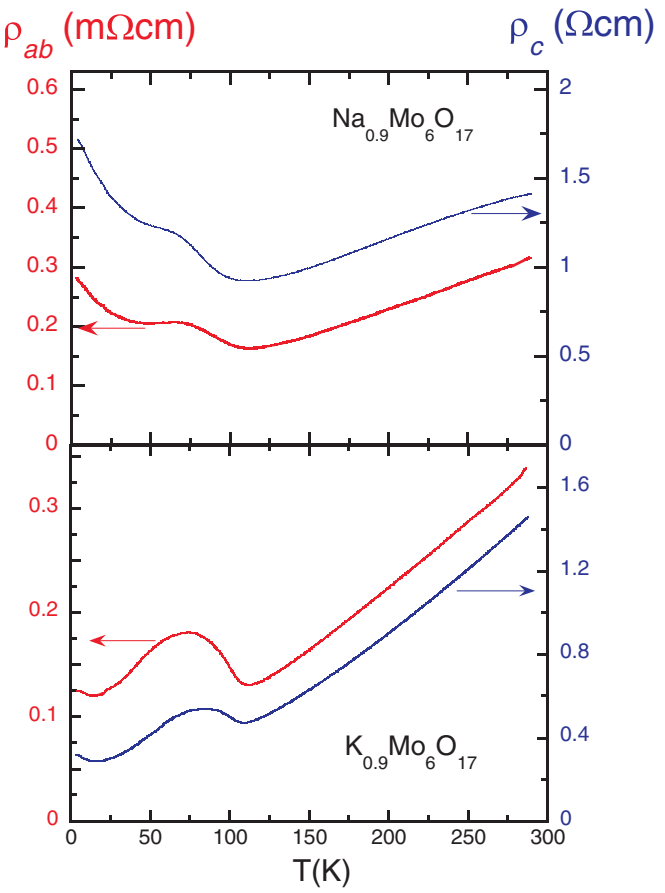

FIG. 1. (Color online) The zero-field in-plane (left axis) and interplane (right axis) resistivity of $Na_{0.9}Mo_6O_{17}$ (top panel) and $K_{0.9}Mo_6O_{17}$ (bottom panel) as a function of temperature between 4.2 and 300 K. The large anisotropy is evident from their different y-axis scales.

In addition to the similarities highlighted above, there are also some notable differences between our measurements and those reported in the literature. While the ρ_c values of both systems are comparable with earlier reports, the absolute values of ρ_{ab} are roughly one order of magnitude lower, making the corresponding resistivity anisotropy (∼3000–4000) significantly higher than previously reported. We attribute these lower in-plane resistivity values to an improved shorting out of the highly resistive interplane current paths. This was achieved by ensuring that the voltage and current contact pads cover the entire thickness of the crystal. If this is not done carefully,

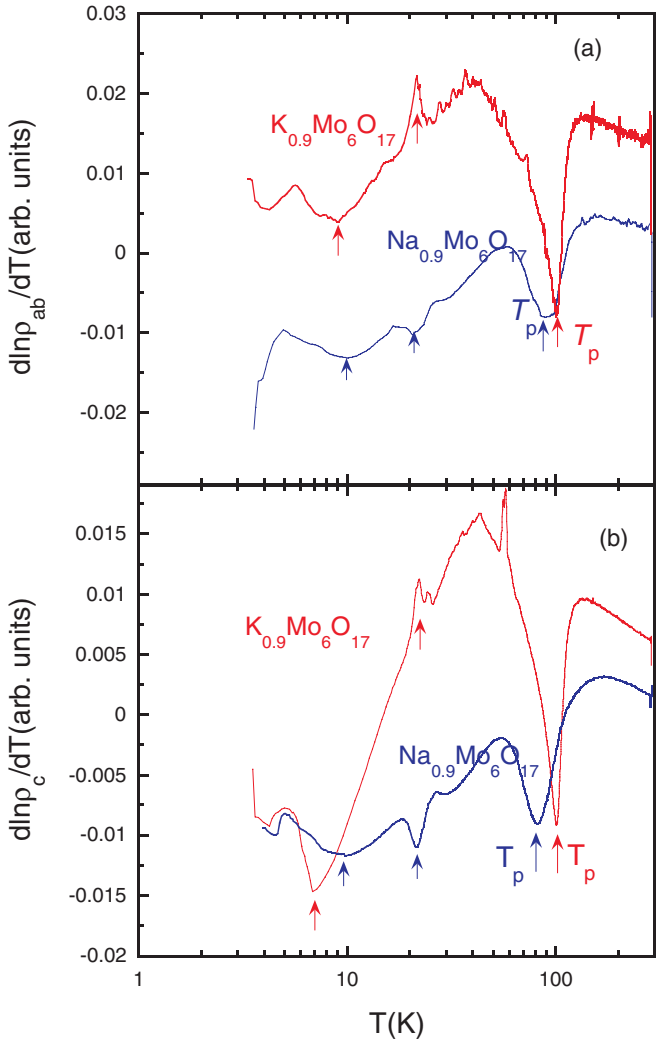

FIG. 2. (Color online) Panels (a) and (b) plot $(d \ln \rho_{ab})/dT$ and $(d \ln \rho_c)/dT$, respectively, to identify the temperature and the width of the CDW transition. In addition to the main CDW transition at T_P, there exist extra structures at low temperature, pointed out by the color-coded arrows, which may be linked to other subdominant CDW/SDW transitions.

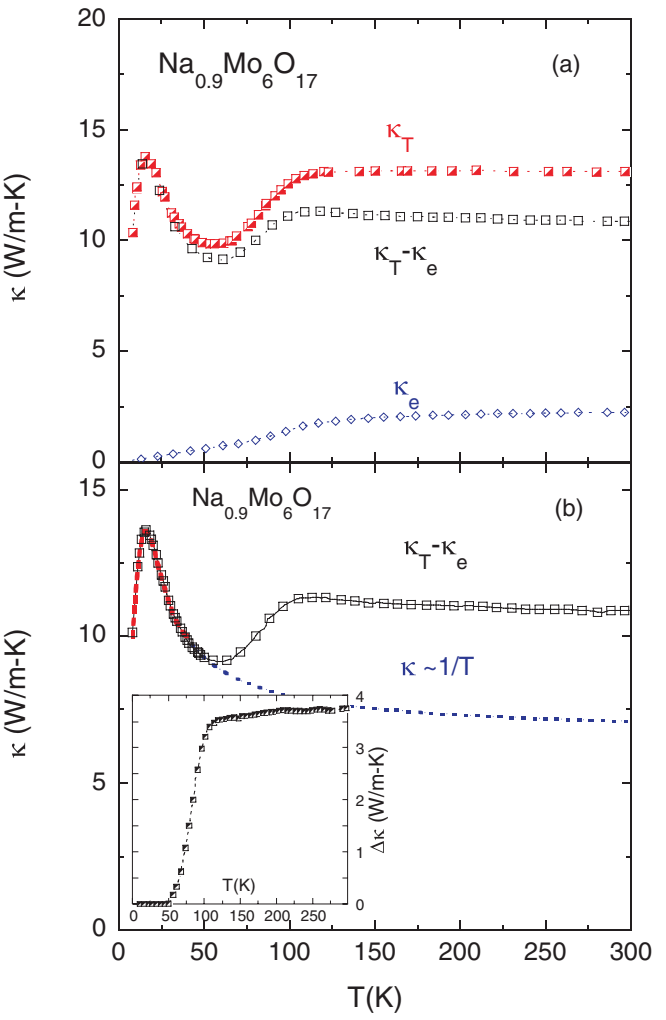

FIG. 3. (Color online) The red two-tone squares in (a) represent the temperature dependence of the total thermal conductivity of $Na_{0.9}Mo_6O_{17}$, as measured directly from the experiments. The blue open circles give the electronic part as determined from their electrical conductivity and the Wiedemann-Franz law, leaving the residual part $\kappa_T - \kappa_e$, as indicated by the black open squares and replotted in panel (b) accordingly, correspond to the contributions from all other excitations. The red solid line in panel (b) indicates the fits to the phonon Boltzmann transport theory (see text). The phonon thermal conductivity κ_{ph}, indicated by the blue dotted line, evolves as $\sim 1/T$ at high temperature. A well-defined excess to κ_{ph}, as plotted in the inset, is clearly evident around and above T_P.

any current flow perpendicular to the conducting planes will lead to a much larger apparent resistivity being measured. We have used this method previously to successfully isolate the low-resistivity direction in a variety of low-dimensional materials and refer the interested reader to our recent work on the Q1D superconductor from the same family ($Li_{0.9}Mo_6O_{17}$), in which we again found a significantly lower resistivity than had been previously reported.[16] Significantly, in that case, the resulting in-plane resistive anisotropy (i.e., for currents parallel and perpendicular to the conducting chains) was found to be consistent with that obtained independently from both optical spectroscopy measurements and the measured upper critical field anisotropy. Such good agreement highlights the efficacy of our technique in isolating the individual components of the conductivity tensor of highly anisotropic systems.

The origin of the second resistive upturn in both bronzes at low temperatures is still unresolved, with spin-density-wave (SDW) formation, a second CDW transition, and localization all put forward as possibilities. Significantly, in $Li_{0.9}Mo_6O_{17}$, a similar upturn is also seen,[18] although in this case, the excellent scaling observed in the longitudinal intrachain magnetoresistance[19] is considered to point more toward some form of DW gapping than localization.

The total in-plane thermal conductivity κ_{ab} as a function of temperature is plotted as red two-tone squares in Figs. 3(a) and 4(a) for $Na_{0.9}Mo_6O_{17}$ and $K_{0.9}Mo_6O_{17}$, respectively. Compared to the zero-field resistivities, which have similar magnitudes and overall display similar behavior (bar the size of the resistive upturn), the in-plane thermal conductivities of the two systems show some notable differences. In $Na_{0.9}Mo_6O_{17}$, $\kappa_{ab}(T)$ is nearly T independent above T_P, then as T cools

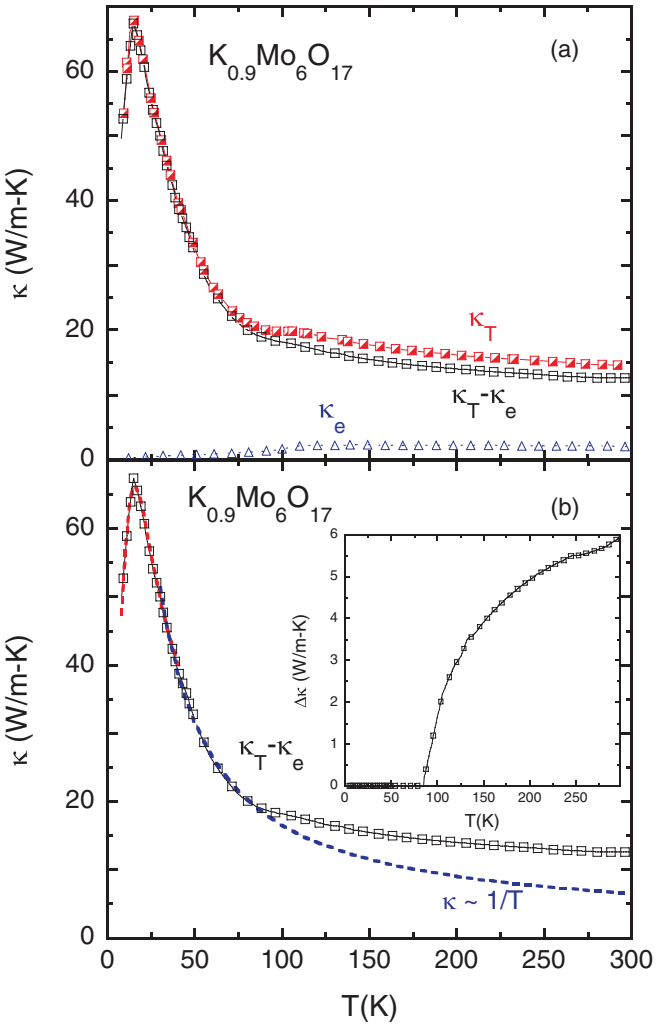

FIG. 4. (Color online) Analogous to Fig. 3, the total thermal conductivity κ_T of $K_{0.9}Mo_6O_{17}$ as measured from the experiments is decomposed into the electronic part κ_e and the residual part $\kappa_T - \kappa_e$ in panel (a). Again, the phonon Boltzmann transport theory was applied to fit the low-T $\kappa_T - \kappa_e$ data, as indicated by the red solid curve in panel (b). A well-defined excess to the phonon thermal conductivity κ_{ph}, which is characteristic of $\sim 1/T$ decay at high temperature and shown by the blue dashed line, is plotted in the inset and evidently seen around and above T_P.

below T_P, $\kappa_{ab}(T)$ first develops a well-defined downturn, goes through a minimum around 50 K, then finally peaks at around 15 K. The thermal conductivity of $K_{0.9}Mo_6O_{17}$, on the other hand, while showing a slight kink at $T \sim 120$ K, increases significantly below T_P, reaching a peak value at $T = 20$ K, which is approximately four times higher than that of $Na_{0.9}Mo_6O_{17}$. The low-temperature peak is typical of the thermal response of phonons and results from the competition between increasing numbers of propagating phonons (with increasing T) and the concomitant reduction of their mean-free path. The larger magnitude of the peak amplitude of κ_{ab} below T_P in $K_{0.9}Mo_6O_{17}$ compared with $Na_{0.9}Mo_6O_{17}$ again reflects a lower level of static disorder in the former.

The total thermal conductivity of a metal consists of the contributions from free carriers, lattice vibrations, and other possible excitations. The electronic component κ_e in an ordinary metal can be estimated from the Wiedemann-Franz law[20]

$$\kappa_e/\sigma T = L_0, \tag{1}$$

where σ is the dc electrical conductivity and $L_0 = 2.45 \times 10^{-8}$ $W\Omega K^{-2}$ is the so-called Lorenz number. Although deviations in this relation are observed in most metals at intermediate temperatures, due to the differing effects of small- and large-angle scattering on the electrical and thermal conductivities, these are typically only of order 20%–30% and, as a first approximation, they can be ignored.

The blue open circles in Figs. 3(a) and 4(a) represent the electronic contribution κ_e, calculated from Eq. (1) and the electrical resistivity data plotted in Fig. 1. The kinks in κ_e of both systems at $T = T_P$ result primarily from the substantial decrease of the carrier density at the CDW transition. The residual part $\kappa_T - \kappa_e$, as replotted in Figs. 3(b) and 4(b) accordingly, thus represents the contributions to the thermal conductivity arising from phonons and any other excitations. Note that the slight kink in $\kappa_{ab}(T)$ of $K_{0.9}Mo_6O_{17}$ is effectively removed once κ_e is subtracted from the raw data. By contrast, for $Na_{0.9}Mo_6O_{17}$, the kink is still very much evident even after subtraction of κ_e. It is important to note that this difference is not simply due to our overestimate of κ_{ab} since we obtained κ_{ab} values of a similar magnitude on a second crystal, nor to any possible underestimate of σ_{ab}. Indeed, in order to remove the kink in $\kappa_T - \kappa_e$ completely, we would have had to underestimate σ_{ab} by a factor of 5, i.e., by an amount more than one order of magnitude greater than our experimental uncertainty (of order 30%). Moreover, the magnitude of σ_{ab} that we measure is already one order of magnitude higher than in previous reports. We are confident therefore that this kink is an intrinsic feature of $\kappa_{ab}(T)$ in $Na_{0.9}Mo_6O_{17}$.

The main component of $\kappa_T - \kappa_e$ is the contribution from the phonons. In our subsequent analysis, we employ the Debye model for the phonon Boltzmann transport theory:[21]

$$\kappa_{ph} = \frac{1}{2\pi^2 \upsilon} \int_0^{\omega_{\max}} \hbar\omega^3 \tau \frac{(\hbar\omega/k_B T^2)\exp(\hbar\omega/k_B T)}{[\exp(\hbar\omega/k_B T) - 1]^2} d\omega, \tag{2}$$

where ω is the phonon frequency, $\omega_{\max}$ is the maximum phonon frequency related to the Debye temperature Θ_D via $\hbar\omega_{\max} = k_B\Theta_D$, $\upsilon = \Theta_D(k_B/\hbar)(6\pi^2 n)^{-1/3}$ is the mean sound velocity with n the number density of atoms, while τ is the phonon relaxation time, which takes account of all the phonon scattering mechanisms. We assume here that these individual scattering processes act independently so that $\tau_\Sigma^{-1} = \Sigma\tau_i^{-1}$, where τ_i corresponds to each individual relaxation time. The main phonon scattering mechanisms come from scattering off two-dimensional defects and phonon-phonon scattering, that is,[22]

$$\tau_\Sigma^{-1} = A\omega^2 + B\omega^2 T \exp(-\Theta_D/bT). \tag{3}$$

In the same way that the quasiparticle mean-free path ℓ can not become shorter than the interatomic spacing a (the so-called Mott-Ioffe-Regel limit[23]), we follow the procedure of Kordonis *et al.* and assume here that the *phonon* mean-free path must also have a lower limit $\ell_{\min}$ with $\tau = \max(\tau_\Sigma, \ell_{\min}/\upsilon)$.[22] We thus set the parameters A, B, and b and $\ell_{\min}$ as freely adjustable parameters and use the Debye temperature extracted from low-T heat-capacity data, as shown below,

TABLE I. Fitting parameters to Eq. (2) with the relaxation time of the form of Eq. (3). $\ell_{\min}$ corresponds to the low boundary of phonon mean-free path (see text).

Parameter	$Na_{0.9}Mo_6O_{17}$	$K_{0.9}Mo_6O_{17}$
$A(10^{-16}$ s)	0.68	0.25
B (10^{-17} s K^{-1})	1.69	0.76
b	10.29	6.06
$\ell_{\min}$ (Å)	158	208
Temperature region (K)	8–40	8–50

to obtain the resultant fitting curves displayed as solid red lines in Figs. 3(b) and 4(b) for $Na_{0.9}Mo_6O_{17}$ and $K_{0.9}Mo_6O_{17}$, respectively. The corresponding fitting parameters are listed in Table I. The values for A, B, and b are typical for κ_{ph} in oxide systems. The values for $\ell_{\min}$, on the other hand, are rather large, although as mentioned by Kordonis *et al.*,[22] the inclusion of $\ell_{\min}$ has little bearing on the fitting of the low temperature $\kappa_{ph}(T)$. Above the fitting range, we assume the typical $1/T$ decay in the phonon thermal conductivity due to phonon-phonon scattering. These tails are depicted in Figs. 3(b) and 4(b) as dashed blue lines.

As mentioned above, the most striking feature of the $\kappa_T - \kappa_e$ data for $Na_{0.9}Mo_6O_{17}$ shown in Fig. 3(b) is the enhancement of the thermal conductivity beginning at around $T = 50$ K. This enhanced conductivity, plotted in the inset of Fig. 3(b), is reminiscent of that seen in other CDW systems such as $(NbSe_4)_{10}I_3$, $K_{0.3}MoO_3$, and $(TaSe_4)_2I$,[24,25] for which it was attributed to the emergence of phason excitations associated with the CDW transition. Note that in these other CDW systems, this contribution exists both above and below T_P, where it typically peaks. The contribution above T_P is considered to arise from fluctuations associated with the phason excitations. Moreover, as noted by Smontara *et al.*,[25] the phason fluctuations may extend to very high temperature due to slow decay of the damping rate Γ. Hence, while we do not expect that phason excitations account for the full excess of thermal conductivity in $Na_{0.9}Mo_6O_{17}$, they may well account for a significant proportion of it.[26] A similar enhancement can also be inferred, although less convincingly, in the thermal conductivity data of $K_{0.9}Mo_6O_{17}$ plotted in the inset of Fig. 4(b) from extrapolation of the $1/T$ decay to higher temperature [dotted curve in Fig. 4(b)]. Note that it is not possible to fit the full $\kappa(T)$ data of $K_{0.9}Mo_6O_{17}$ using Eq. (2), and that a fit to the high-T $\kappa(T)$ data incorporating $\ell_{\min}$ gives unphysical values for A, B, and b and strongly underestimates the enhancement in $\kappa(T)$ below T_P.

The specific heat $C_p(T)$ data, shown in Figs. 5 and 6, uncover another marked difference between the two systems. For $K_{0.9}Mo_6O_{17}$, a large, well-defined heat-capacity anomaly, clearly associated with the CDW transition, is observed. The anomaly shown in Fig. 6(a) is in fact much sharper than has been reported previously.[4] By contrast, the corresponding feature in $Na_{0.9}Mo_6O_{17}$ is extremely broad and, as such, is difficult to pinpoint. In contrast with the resistivity data, no additional anomalies could be found at lower temperatures in either system due to any putative subdominant CDW/SDW transitions. A magnetic field of 14 T is found to have no effect on the shape or position of the specific heat anomaly in both systems.

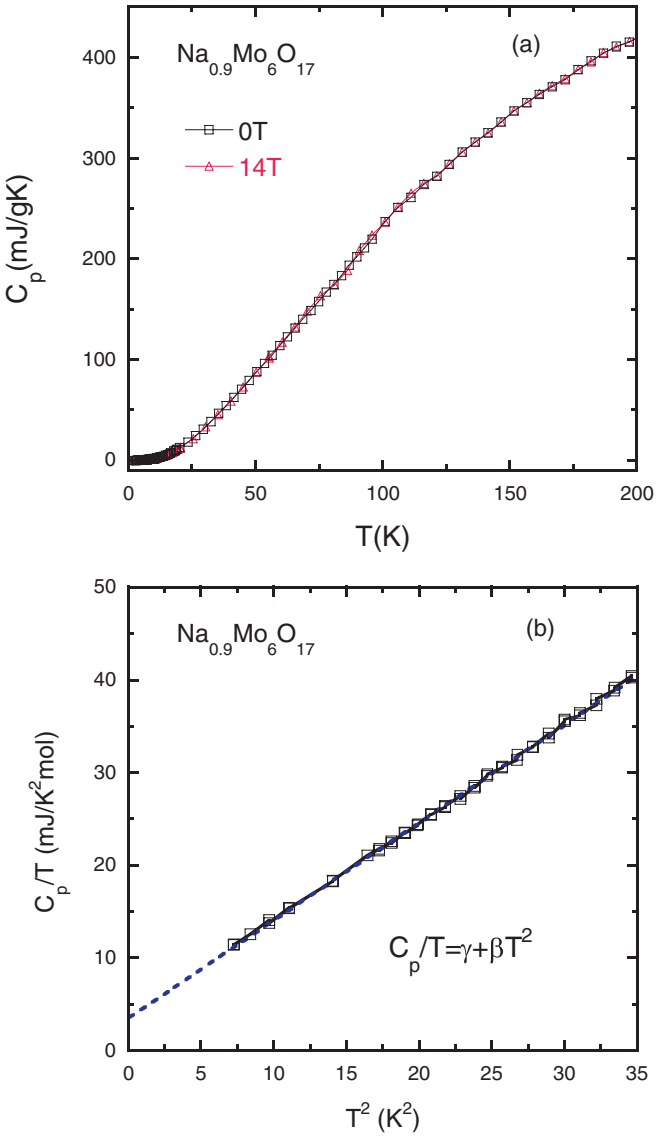

FIG. 5. (Color online) (a): The temperature dependence of the specific heat in both zero field (black square) and 14-T magnetic field (red triangle) of $Na_{0.9}Mo_6O_{17}$. Evidently, an applied magnetic field has little effect on its overall heat capacity. (b): The low-temperature zero-field C_P/T data plotted as a linear function of T^2 to allow the normal electronic and acoustic phonon contributions to the specific heat to be delineated. The fitting gives $\gamma = 3.57$ mJ/K^2 mol, $\beta = 1.05$ mJ/K^4 mol.

Plots of C_p/T versus T^2 at the lowest temperature allow us to separate out the electronic ($=\gamma T$) and phononic ($=\beta T^3$) contributions, as shown in of Figs. 5(b) and 6(b). From the extracted γ values, given in the figure caption, we determine the density of states of normal carriers at the Fermi level to be 1.515 eV^{-1} per molecule and 0.275 eV^{-1} per molecule for $Na_{0.9}Mo_6O_{17}$ and $K_{0.9}Mo_6O_{17}$, respectively. Debye temperatures of 333 and 228 K for $Na_{0.9}Mo_6O_{17}$ and $K_{0.9}Mo_6O_{17}$, respectively, can also be estimated from the formula $\Theta_D^3 = \frac{5}{12}\pi^4 r R \beta^{-1}$ with R the gas constant and r the total number of atoms in one formula unit ($r = 24$ for both cases). We note that the Θ_D value extracted here for $K_{0.9}Mo_6O_{17}$ is somewhat lower than those reported in the literature.[27,28]

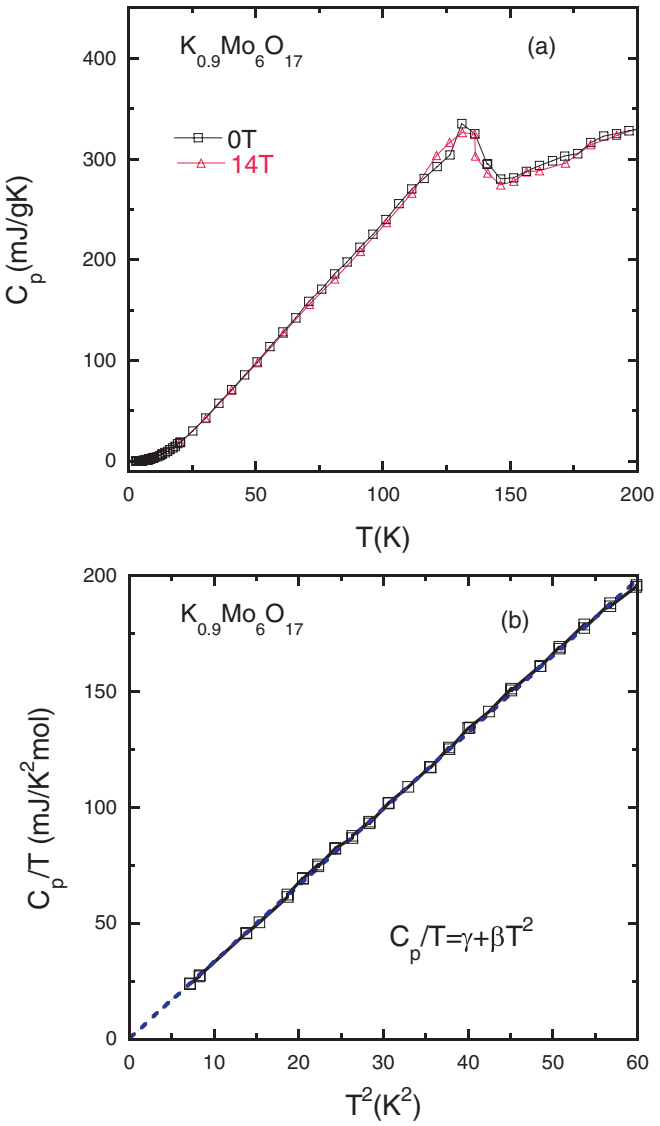

FIG. 6. (Color online) Similar to Fig. 5, panel (a) shows the temperature dependence of the specific heat in both zero field (black square) and 14-T magnetic field (red triangle) of $K_{0.9}Mo_6O_{17}$. As noted, an applied magnetic field has little effect on the total heat capacity. Panel (b) separates the normal electronic and acoustic phonon contributions by fitting C_P/T of $H = 0$ T data as a linear function of T^2 at very low temperatures. The resultant fitting parameters are $\gamma = 0.65$ mJ/K^2 mol, $\beta = 3.30$ mJ/K^4 mol.

IV. DISCUSSIONS AND CONCLUSION

In many CDW compounds, the thermal conductivity is enhanced substantially below the Peierls transition, as a result of changes in the electron- or phonon-scattering processes. However, in other CDW compounds, such as $(NbSe_4)_{10}I_3$, $K_{0.3}MoO_3$ and $(TaSe_4)_2I$,[24,25] the thermal conductivity is observed to pass through a well-defined minimum below the Peierls transition before increasing again at lower temperatures. It has been proposed that this additional contribution results from phason modes with large velocity.[25] Given the strong similarity in the behavior of $\kappa_{ab}(T)$ in $Na_{0.9}Mo_6O_{17}$ with those systems listed above, it would seem appropriate to ascribe at least part of the excess thermal conductivity shown in the inset of Fig. 3(b) to the same origin.

While there is no well-defined minimum in $\kappa_{ab}(T)$ in $K_{0.9}Mo_6O_{17}$ in the region of the Peierls transition, inspection of Fig. 4(b) reveals a small excess thermal conductivity above the high-T $1/T$ decay of κ_{ph}, which could correspond to the same phason contribution seen much more clearly in $Na_{0.9}Mo_6O_{17}$. Evidence for phason excitations from measurements of the low-temperature specific heat of $K_{0.9}Mo_6O_{17}$ was claimed in Ref. 28 through the observation of a broad hump in C/T^3 around $T = 16$ K. Given that this temperature coincides with the onset of the low-temperature upturn in the resistivity of $K_{0.9}Mo_6O_{17}$, it is not yet clear whether this feature can be ascribed unambiguously to phasons or to a second density-wave transition.

The origin of the striking difference in the thermoelectric power of the Q2D purple bronzes below $T = T_P$, as described briefly in the Introduction, remains to be resolved, although it is likely to arise from subtle differences in the electronic structure, as hinted at by ARPES,[6,7] as well as in the relative mobilities of the carriers on the remnant Fermi surface(s). According to Breuer *et al.*,[7] the Fermi surface in $Na_{0.9}Mo_6O_{17}$ comprises an elliptical electron pocket, i.e., around the Γ point, which is less prone to nesting, and a diamond-shaped hole pocket with flat regions that are highly susceptible to nesting. The negative thermopower below T_P in $Na_{0.9}Mo_6O_{17}$ is therefore consistent with the notion that the remnant Fermi surface below T_P will be predominantly located about the more-rounded sections of the single electron pocket.

The second electron pocket found in $K_{0.9}Mo_6O_{17}$ uncovered by Gweon *et al.*[6] is starlike. Intriguingly, between the apices of the stars lie rounded regions of Fermi surface with *negative* curvature, i.e., that are centered around the edges of the Brillouin zone rather than around its center. Hence, while the second pocket in $K_{0.9}Mo_6O_{17}$ is electronlike, those regions unaffected by the CDW transition will have predominantly holelike character. In the heavily overdoped cuprate $La_{2-x}Sr_xCuO_4$ ($x = 0.30$), which also has an electron pocket with regions of negative curvature, a similar inversion of the sign of the thermopower[29] and of the Hall coefficient[30] is observed. In this regard, it would be very interesting to explore the evolution of the in-plane Hall coefficient in both purple bronzes above and below T_P.

One of the most notable findings of this study is the observation that the Q2D purple bronzes $Na_{0.9}Mo_6O_{17}$ and $K_{0.9}Mo_6O_{17}$ display distinct transport and thermodynamic properties associated with their CDW transitions. Given the possible differences in the Fermiologies of the two systems, as inferred by ARPES,[6,7] and their very different thermoelectric responses below $T = T_P$,[10] as described above, these differences might, on first inspection, suggest that the nature and mechanisms of CDW formation in these two Q2D bronzes are in fact distinct. However, we argue here that a more consistent explanation of these contrasting behaviors can be provided by considering the different crystal chemistries of the two systems and the resulting variation in disorder content.

Regarding the latter, we note from the high-temperature T-linear resistivities plotted in Fig. 1 that the extrapolated residual resistivity in $Na_{0.9}Mo_6O_{17}$ is significantly higher than in $K_{0.9}Mo_6O_{17}$. Moreover, the low-T resistivity in the Na

bronze is approximately twice that at the resistive minimum, while in $K_{0.9}Mo_6O_{17}$, it remains comparable, even though the low-T heat capacity data reveal that the density of states in $Na_{0.9}Mo_6O_{17}$ is substantially higher below T_P. This comparison implies that the A = Na bronze is significantly more susceptible to localization effects, an indicator of higher levels of disorder scattering. This conclusion is further corroborated by the observation that the peak in the phonon thermal conductivity at low temperatures, a quantitative measure of the phonon mean-free path, is approximately four times lower in $Na_{0.9}Mo_6O_{17}$ than in $K_{0.9}Mo_6O_{17}$. This argument is also consistent with what was seen in Fig. 2 where the width of negative peak of $(d \ln \rho)/dT$ at T_P, a strong indicator of disorder level, is much narrower in $K_{0.9}Mo_6O_{17}$. Finally, the anomaly in the heat capacity, while sharp in our $K_{0.9}Mo_6O_{17}$ crystal, is smeared out in the Na-doped counterpart. A similarly broad heat-capacity anomaly was also reported for $K_{0.9}Mo_6O_{17}$ almost three decades ago[4] in crystals grown by a different group, although unfortunately, there is no accompanying transport data in that study to allow us to compare their residual resistivities directly. Nevertheless, such variation in the heat-capacity anomaly in what are nominally the same compound does suggest that there is indeed a strong sample dependence in the thermodynamic properties of the two systems.

The $Na_{0.9}Mo_6O_{17}$ system is known to possess a variable Na content.[17] Variation in stoichiometry in the sodium purple bronzes is usually considered to be a characteristic that exists between crystals, rather than within an individual crystal. However, given the higher mobility of sodium atoms within the melt relative to that of the potassium, we speculate here that there may be more of a tendency for the Na ions to form clusters within each crystal, which in turn will lead to enhanced elastic scattering of the quasiparticles on the conducting molybdate chains. It is also noted that clustering of Na ions may lead to a distribution of transition temperatures and therefore increase the breadth of the transition, as indeed seen in Fig. 2. However, a distribution of concentration could yield a distribution of the Fermi vectors in different parts of the crystal, favoring the incommensurate character of the CDW, a necessary condition to have phasons, which does not seem to be fulfilled in $K_{0.9}Mo_6O_{17}$.

In summary, we have studied the transport and thermodynamic properties of two Q2D purple bronzes $Na_{0.9}Mo_6O_{17}$ and $K_{0.9}Mo_6O_{17}$ and have revealed significant differences in their physical properties above and below their CDW transitions. These differences appear to arise from differences in their stoichiometry, possibly caused by the volatility of sodium during crystal growth. An unusual enhancement of the thermal conductivity has been attributed, in comparison with other CDW systems, to the possible emergence of phason excitations in these two systems. Finally, measurements of the electrical resistivity reveal an electrical anisotropy that is one order of magnitude larger than previously thought.

ACKNOWLEDGMENTS

The authors would like to acknowledge technical assistance from B. Fauqué, X. Y. Tee, and helpful discussions with J. D. Fletcher and N. Shannon. This work was supported by the National Natural Science Foundation of China (Grant No. 11104051), the EPSRC (UK), the Royal Society and the National Research Foundation, Singapore. X.X. would also like to acknowledge the financial support from Department of the Education Office of Zhejiang Province, China (Grant No. Y200907686).

[1] P. A. Lee, T. M. Rice, and P. W. Anderson, Solid State Commun. **14**, 703 (1974).
[2] H. Fröhlich, Proc. R. Soc. London, Ser. A **223**, 296 (1954).
[3] M. Greenblatt *et al*., Chem. Rev. **88**, 31 (1988).
[4] C. Escribe-Filippini *et al*., Philos. Mag. B **50**, 321 (1984).
[5] P. Mallet, K. M. Zimmermann, P. Chevalier, J. Marcus, J. Y. Veuillen, and J. M. Gomez Rodriguez, Phys. Rev. B **60**, 2122 (1999).
[6] G. H. Gweon, J. W. Allen, J. A. Clack, Y. X. Zhang, D. M. Poirier, P. J. Benning, C. G. Olson, J. Marcus, and C. Schlenker, Phys. Rev. B **55**, R13353 (1997).
[7] K. Breuer, C. Stagarescu, K. E. Smith, M. Greenblatt, and K. Ramanujachary, Phys. Rev. Lett. **76**, 3172 (1996).
[8] M. H. Whangbo, E. Canadell, and C. Schlenker, J. Am. Chem. Soc. **109**, 6308 (1987).
[9] M. H. Whangbo, E. Canadell, P. Foury, and J. P. Pouget, Science **252**, 96 (1991).
[10] M. L. Tian *et al*., Phys. Lett. A **234**, 477 (1997).
[11] M. L. Tian *et al*., J. Appl. Phys. **89**, 3408 (2001).
[12] M. L. Tian *et al*., J. Phys.: Condens. Matter **13**, 311 (2001).
[13] M. Tian, S. Yue, and Y. Zhang, Phys. Rev. B **65**, 104421 (2002).
[14] M. Greenblatt *et al*., J. Solid State Chem. **59**, 149 (1985).
[15] N. Wakeham, A. F. Bangura, X. Xu. M. Greenblatt, and N. E. Hussey, Nat. Commun. **2**, 396 (2011).
[16] J.-F. Mercure *et al*. (unpublished).
[17] K. V. Ramanujachary, M. Greenblatt, and W. H. McCarroll, J. Cryst. Growth **70**, 476 (1984).
[18] M. Greenblatt *et al*., Solid State Commun. **51**, 671 (1984).
[19] X. Xu *et al*., Phys. Rev. Lett. **102**, 206602 (2009).
[20] N. W. Ashcroft and N. D. Mermin, *Solid State Physics* (Cornell University Press, New York, 1975).
[21] R. Berman, *Thermal Conduction in Solids* (Clarendon, Oxford, UK, 1976).
[22] K. Kordonis, A. V. Sologubenko, T. Lorenz, S. W. Cheong, and A. Freimuth, Phys. Rev. Lett. **97**, 115901 (2006).
[23] N. E. Hussey, K. Takenaka, and H. Takagi, Philos. Mag. **84**, 2847 (2004).
[24] R. S. Kwok and S. E. Brown, Phys. Rev. Lett. **63**, 895 (1989).
[25] A. Smontara, K. Biljakovic, and S. N. Artemenko, Phys. Rev. B **48**, 4329 (1993).
[26] K. Biljakovic, J. C. Lasjaunias, F. Zougmore, P. Monceau, F. Levy, L. Bernard, and R. Currat, Phys. Rev. Lett. **57**, 1907 (1986).
[27] J. Wang, R. Xiong, D. Yin, C. Li, Z. Tang, Q. Wang, J. Shi, Y. Wang, and H. Wen, Phys. Rev. B **73**, 193102 (2006).
[28] R. Buder *et al*., J. Phys. (Paris), Lett. **43**, L59 (1982).
[29] Y. Nakamura and S. Uchida, Phys. Rev. B **47**, 8369 (1993).
[30] A. Narduzzo, G. Albert, M. M. J. French, N. Mangkorntong, M. Nohara, H. Takagi, and N. E. Hussey, Phys. Rev. B **77**, 220502(R) (2008).